Journal of Biomedical Optics 9(3), 474–480 (May/June 2004)

Optical biopsy of bone tissue: a step toward the diagnosis of bone pathologies

Antonio Pifferi
Alessandro Torricelli
Paola Taroni
Andrea Bassi
Ekaterine Chikoidze
Eleonora Giambattistelli
Rinaldo Cubeddu
ULTRAS-INFM and IFN-CNR, Dipartimento di Fisica—Politecnico di Milano,
Piazza Leonardo da Vinci 32, I-20133 Milan, Italy

Abstract. *In vivo* absorption and reduced scattering spectra of the human calcaneous from 650 to 1000 nm were assessed using a laboratory system for time-resolved transmittance spectroscopy. Measurements were performed on the calcaneous of seven female volunteers ranging from 26 to 82 years of age. The analysis of the absorption spectra, using a linear combination of the key tissue absorbers (bone mineral, water, lipids, oxy- and deoxyhemoglobin), revealed a general decrease in bone mineral content and an increase in lipids with age, which is in agreement with the aging transformations that occur in bone tissues. The scattering spectra were less effective in detecting such changes in older subjects, showing only a minor decrease in the coefficient for these subjects. The capability to noninvasively quantify bone tissue composition suggests a possible use of optical biopsy for the diagnosis of bone pathologies such as osteoporosis, which are characterized by a progressive reduction and transformation of the mineral in the bone matrix. [DOI: 10.1117/1.1691029]

Keywords: photon migration, time-resolved spectroscopy, bone, osteoporosis, optical biopsy.

Paper 044015 received Jul. 28, 2003; revised manuscript received Dec. 19, 2003; accepted for publication Dec. 19, 2003.

1 Introduction

Osteoporosis as a multifactorial disease is a major public health problem: 1 of 3 women and 1 of 12 men over the age of 50 have osteoporosis, and every 3 min someone in the world has a fracture that is due to osteoporosis.[1] It is a disease in which the amount of bone is decreased and its structural integrity impaired. Osteoporosis literally means ''porous bones''; the holes inside a bone become bigger, making it fragile and liable to break easily.[2,3] It usually affects the whole skeleton, but most commonly causes fractures to the wrist, spine, and hip. The consequences include decreased functional independence. The lifetime risk, owing to immobilization, is significant, and the related social costs are huge and expected to increase even more as the population grows older.

An understanding of the differences in types of bone and the units of measurement is important for drawing conclusions about available techniques for characterizing bone and diagnosing osteoporosis, and more generally for judging study results and patient data. Bone plays a vital role as a mineral reservoir and source of hematopoietic cells. Moreover, it is unique with respect to other structural materials in that it can undergo self-repair and can adapt its composition and structure in response to hormonal and mechanical stimuli. Bone in humans and other mammals is generally classified into two types: (1) cortical bone, also known as compact bone, and (2) trabecular bone, also known as cancellous or spongious bone. These two types are distinguished on the basis of porosity and microstructure.[4] Cortical bone is much denser, with a porosity ranging between 5 and 10%. It is found primarily in the shaft of long bones and forms the outer shell around cancellous bone at the end of joints and vertebrae. The hard compact bone also protects the marrow, which is located inside the compact bone and, besides red and white cells, contains fat. Trabecular bone, with a porosity ranging anywhere from 50 up to 90%, is found in the end of long bones, in vertebrae, and in flat bones like the pelvis.

The structural components of bone consist of an inorganic matrix (largely mineralized) and an organic matrix. The inorganic matrix contains calcium hydroxyapatite, which is responsible for the compressive strength of bone, and osteocalcium phosphate (brushite). The main components of the organic matrix are collagen, proteins, and blood cells. It is the calcium and phosphorus component of the inorganic matrix that makes bone hard and rigid, and the arrangement of the collagen fibers in the organic matrix that makes it strong. In both men and women, bone mineral loss from the skeleton starts generally at ages 40 to 50. In women bone loss can be rapid immediately after menopause.

Bone strength reflects the integration of two main features: density and quality. Bone mineral density (BMD) is expressed as grams of mineral per area or volume, while bone quality refers to architecture, turnover, and mineralization. In clinical practice, bone mineral density is usually expressed as a T score (number of standard deviations from the young normal mean) or Z score (number of standard deviations from the age-matched mean). T scores between −1 and −2.5 indicate

Address all correspondence to Antonio Pifferi, INFM-Dipartimento di Fisica and INF-CNR, Politecnico di Milano, Piazza Leonardo da Vinci 32, I-20133 Milan, Italy. Tel: +39-02-23996072; FAX: +39-02-23996126; E-mail: antonio.pifferi@fisi.polimi.it

1083-3668/2004/$15.00 © 2004 SPIE

low bone mass or osteopenia. T scores below −2.5 indicate osteoporosis.[5–8]

At present several methods are available to measure bone density. During the past 10 years, dual-energy x-ray absorptiometry (DEXA) has emerged as a cost-effective and accurate means to quantify skeletal mass. Because bone strength and resistance to fracture depend, not only on the amount of mineral present, but also on the three-dimensional conformation (bone quality), some investigators have questioned the accuracy of BMD measurements in predicting fracture risk.[9–11] Ultrasound is used to discriminate normal from osteopenic bone without exposing the patient to ionizing radiation. Several methods have been developed that variously examine the speed, the attenuation, or the reflection of ultrasounds. The interest in their use is due to the information they provide concerning the structural organization of bone in addition to bone mass or density. However, it is not yet known whether the ultrasound attenuation and the speed of sound provide a measure of bone quality and an assessment of bone fragility.[12–14]

Other techniques (x-ray photon scattering methods, neutron activation) for measuring bone mineral have been developed, but their current use is largely confined to clinical research.[15] Recently, it has been reported that magnetic resonance imaging (MRI) may discriminate normal from osteopenic bone.[16] Moreover, this modality may provide additional data, such as trabecular thickness and microarchitectural factors. However, the high cost and complexity of MRI examinations make it unfeasible to replace standard DEXA measurements with more advanced MRI analysis. Optical biopsy is potentially an interesting tool for probing bone and joints pathologies because of its inherent noninvasiveness and the high informative content encoded in the spectral differentiation of tissue constituents. However, the diffusive nature of biological tissues and their strong attenuation even for a thickness of a few centimeters hampers a direct estimate of tissue absorption properties using standard techniques. Initial studies have demonstrated the feasibility of optical tomography for the reconstruction of optical properties in finger joints, with interesting potentialities for the diagnosis of arthritis.[17,18]

On the problem of osteoporosis, an interesting correlation between the bone scattering coefficient and the degree of demineralization was found using light-scattering techniques.[19] These results were obtained *in vitro* on dried and denatured bones, while applicability to the *in vivo* situation and perturbations produced by the organic matrix need to be investigated. Other optical techniques such as like Raman spectroscopy, have been used to study pathological changes of the bone *in vitro*,[20] while their use *in vivo* is hardly feasible.

In this work we used for the first time time-resolved transmittance spectroscopy (TRS) to measure the optical properties of the calcaneous *in vivo* over a wide spectral range. Analysis of the absorption spectra allowed us to estimate the percentage of bone tissue constituents (water, oxy- and deoxyhemoglobin, lipids, and bone mineral), while interpretation of the scattering spectra on the basis of Mie theory yielded the effective density and effective radius of scattering centers. Measurements were performed on the calcaneous because it consists of a trabecular type of bone where pathological changes are revealed earlier, and also because it offers a large bone region with a thickness that is compatible with diffuse transmittance measurements. The goal of our study was to verify the feasibility of the *in vivo* optical characterization of bone components among subjects and to obtain some insight into the physiological changes of bone tissue with age. The possible observation of systematic changes would encourage us to perform future work toward a proper optical spectroscopic diagnosis of pathological changes in bone, such as osteopenia and osteoporosis.

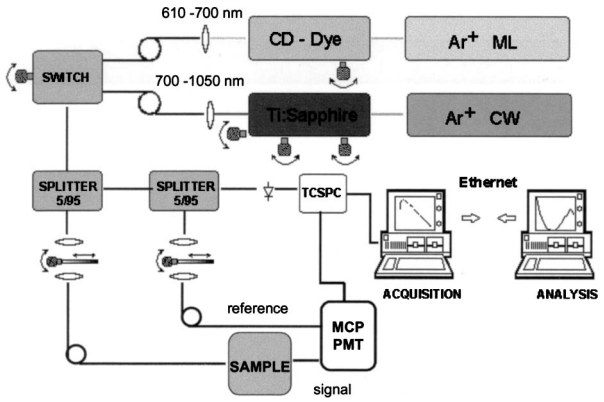

Fig. 1 System setup. CD, cavity-dumped; ML, mode-locked; CW, continuous wave; TCSPC, time-correlated single-photon counting; MCP-PMT, microchannel plate photomultiplier tube.

2 Methods

2.1 *System Setup*

A schematic diagram of the experimental setup is displayed in Fig. 1. A synchronously pumped mode-locked dye (DCM) laser was used as the excitation source from 650 to 695 nm, while an actively mode-locked titanium:sapphire laser provided light in the wavelength range of 700 to 1000 nm.

A 1-mm plastic-glass fiber (PCS1000W, Quartz et Silice, France) delivered light into the tissue and a fiber bundle (5 mm diameter, 1 m length) collected the transmitted photons. The power density at the distal end of the illumination fiber was always kept to less than 10 mW. A double microchannel plate photomultiplier (R1564U with S1 photochatode, Hamamatsu, Japan) and a printed circuit board for time-correlated single-photon counting (SPC130, Becker & Hickl, Germany) were used for detection. A small fraction of the incident beam was coupled to a 1-mm fiber (PCS1000W, Quartz et Silice) and fed directly to the photomultiplier for online recording of the instrumental response function (IRF). Overall, the IRF was $<$120 ps and $<$180 ps FWHM in the red and near-infrared, respectively. Time-resolved transmittance curves were collected in 5-nm steps from 650 to 1000 nm.

2.2 *Analysis of TRS Data*

By fitting the experimental data with a standard solution of the diffusion approximation to the transport equation for a homogeneous slab,[21] we were able to extract the values of the average reduced scattering (μ_s') and absorption (μ_a) coefficients at each wavelength. We used the extrapolated boundary condition[22] and, according to Furutsu and Yamada,[23] the diffusion coefficient $D=1/(3\mu_s')$ was independent of the ab-

sorption properties of the medium. The theoretical curve was convoluted with the IRF and normalized to the area of the experimental curve. The fitting range included all points with a number of counts higher than 80% of the peak value on the rising edge of the curve and 1% on the tail. The best fit was reached with a Levenberg-Marquardt algorithm[24] by varying both μ_s' and μ_a in order to minimize the reduced χ^2.

2.3 *Tissue Composition and Structural Properties*

To evaluate the percentage composition of tissues, the absorption spectra were best fitted with a linear combination of the spectra of the main tissue constituents [i.e., bone minerals, lipid, water, oxy- and deoxyhemoglobin (HbO_2 and HHb)]:

$$\mu_a(\lambda) = \Sigma_i c_i \epsilon_i(\lambda), \tag{1}$$

where λ is the wavelength, c_i is the concentration (a free parameter in the fitting procedure), and $\epsilon_i(\lambda)$ is the specific absorption of the *i*'th constituent. For this purpose, the spectra of water,[25] HHb, and HbO_2[26] were obtained from the literature, while the authors[27] had measured the absorption spectra of lipid (lard) previously. In the present study, the optical spectra of bone, reported in Sec. 3, was measured with our setup. Collagen was not considered as a separate and individual component since its spectral features can barely be distinguished from those of bone, making the fit of absorption spectra less robust when both constituents are included. The knowledge of the absorption properties of the two forms of hemoglobin also allowed us to evaluate the total hemoglobin content $tHb = [HHb] + [HbO_2]$ and the hemoglobin oxygen saturation $SO_2 = [O_2Hb]/\{[HHb] + [HbO_2]\}$.

Further information could be obtained from the reduced scattering spectra. For a homogeneous sphere of radius *r*, Mie theory predicts the wavelength dependence of the scattering and the relation between scattering and sphere size.[28] Under the hypothesis that the scattering centers are homogeneous spheres behaving individually, the relationship between μ_s' and λ can be empirically described as follows:[29]

$$\mu_s'(\lambda) = a\lambda^{-b}, \tag{2}$$

where *a* and *b* are free parameters. In particular, *a* is proportional to the density of the scattering centers, and *b* depends on their size.

2.4 *Measurement Protocol*

In order to study the changes in bone tissue with age, we performed *in vivo* measurements on the calcaneous of seven female volunteers (26, 28, 31, 38, 69, 70, and 82 years old). The subjects were lying on a medical bed and their right or left foot was vertically fixed in a home-built device specially constructed for these measurements, as shown in Fig. 2. According to the standard x-ray diagnostics technique, we chose the following position for the injection fiber and collection bundle: from the lowest point of the Achilles tendon we moved 1.4 cm along the horizontal and vertical directions. The measured thickness of the calcaneous was 4.0 ± 0.3 cm. Total measurement time for each spectrum was about 10 min. For each subject, two spectra for each foot were acquired.

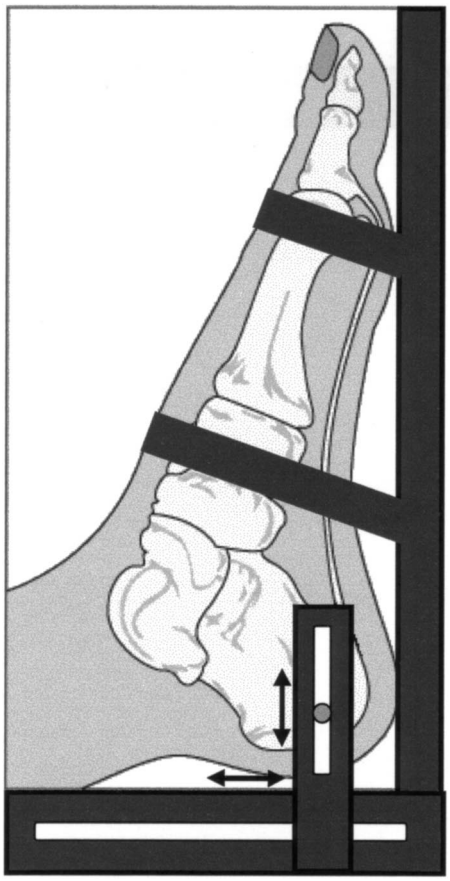

Fig. 2 Positioning of the fibers onto the calcaneous by means of a home-built XY stage.

3 Results and Discussion

To perform a complete analysis of the calcaneous, we needed the optical characterization of all the main components present in the examined tissue. The spectra of water, lipids, oxy- and deoxyhemoglobin are known from the literature, but the spectrum of the mineral in the bone matrix was not available for the whole spectral range. Besides measurements at discrete wavelengths,[19,30] the published spectral data were obtained *in vitro* on a pig skull in the wavelength range 650 to 950 nm.[31] However, these data were obtained on pig skull samples after sonication; thus they still included contributions of water and organic matrix. To derive the absorption properties of the pure mineral in the matrix, we measured the absorption and reduced scattering spectra of dried and denatured bovine bone (Gen-Ox, Brazil).[32] The sample was a parallelepiped of $3 \times 2 \times 2$ cm bearing only the mineral matrix. Figure 3 shows the absorption (black diamonds) and scattering (white diamonds) spectra measured in transmittance geometry along the longest axis. To account for the high porosity of the trabecular bone, the measured absorption coefficient was multiplied by a factor 2.95, which was derived by dividing the effective density of the mineral matrix reported in the literature (1.92 g/cm^3)[33] by the apparent density of the sample (0.65 g/cm^3). The absorption spectrum is characterized by a small shoulder around 915 nm and by a tail at both ends of the spectral range, especially at long wavelengths. The scattering

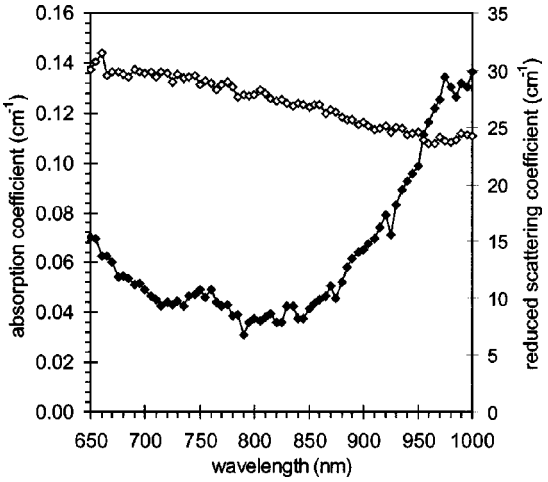

Fig. 3 Absorption spectrum (black diamonds) and reduced scattering spectrum (white diamonds) of bovine dry bone matrix.

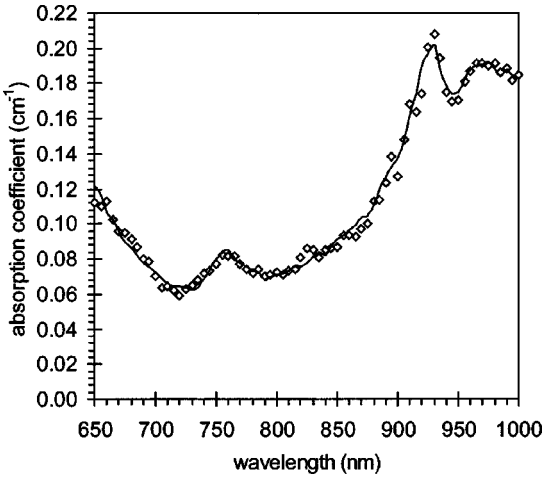

Fig. 5 Absorption spectrum of the right calcaneous for the 38-year-old volunteer. Experimental data (diamonds) and theoretical fitting curve (solid line), using a linear combination of the key tissue constituents.

spectrum is rather flat, which corresponds to large scattering particles. Since scattering interactions are due to changes in the refractive index, it is difficult to compare the scattering spectrum derived on the pure mineral matrix with the *in vivo* spectrum. In fact, in the living bone, the empty spaces caused by demineralization are filled with lipids, water, and collagen, with a refractive index other than air.

Figure 4 presents the absorption spectra of the left calcaneous for three volunteers aged 26, 69, and 82 years, representing the two extremes and an intermediate case. The absorption in the range 650 to 700 nm is due to both hemoglobin and bone mineral. The small peak around 760 nm can be associated with the presence of water, lipids, and deoxyhemoglobin, while the strong peak at 930 nm with values around 0.2 cm^{-1} is due to lipids. With increasing age, the absorption in the region beyond 950 nm, which is due to water and the mineral part of bone, becomes less evident than the lipid peak centered at 930 nm. Also, for the oldest subject, the absorption in the region of $\leqslant$750 nm is significantly higher than in the younger subjects, possibly suggesting higher blood content or lower oxygen saturation.

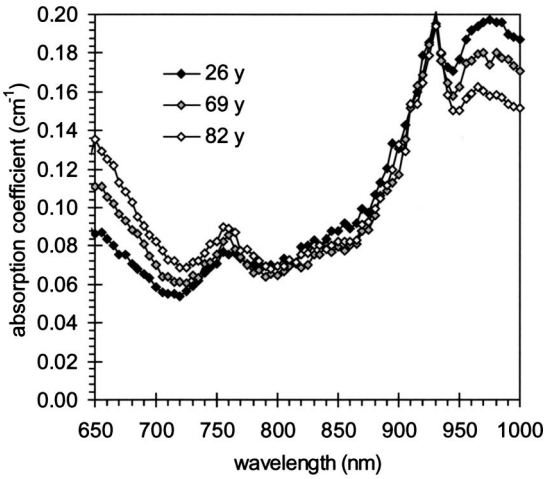

Fig. 4 Average absorption spectra of the left calcaneous for the 26-, 69-, and 82-year-old volunteers.

Figure 5 shows the absorption spectrum of the right calcaneous of the 38-year-old volunteer interpolated using a linear combination of the five tissue components (water, lipids, HHb, HbO_2, and bone mineral). The resulting amount of bone mineral matrix is 16%; the lipid content is 54%, while water contributes 16%. The low amount of bone can be understood if it is remembered that this percentage refers only to the mineral fraction, while most of the ''bone volume'' is filled with lipids. Total hemoglobin content (27 μM) and the tissue oxygen saturation (70%) are in the typical range for human tissues.

This kind of analysis was performed for all subjects, and the results are shown in Fig. 6 for (a) bone mineral, (b) lipids, (c) water, (d) sum of the three main components (bone, water, and lipids), (e) tHb, and (f) SO_2. The mean values and standard deviation for two repeated measurements on both feet (a total of four measurements) are displayed for each subject. The dashed line is the least-squares fit to the data. This is a rough estimate to show a possible trend of mean value with age. However, this does not necessarily imply that we expect a linear trend. Also, owing to wide physiological differences among subjects and the limited number of volunteers, no definite generalization can be drawn from the linear regression. Thus the line will be used here only to point out age-related differences among these seven subjects. Bone mineral matrix decreases for older subjects, which is in agreement with the well-known bone density loss with age, while lipids seem to increase. This result is in agreement with clinical observations that above 40 years of age, when demineralization occurs, lipid substitutes for other components in bone tissue. The trend line shows a decrease in water content with age, although with a high intersubject variation. The sum of water, lipids, and bone mineral content is 80% on average. The fraction remaining to total 100% is possibly due to other constituents (e.g., proteins) that were not considered in the fitting procedure, owing to the low absorption in the 650 to 1000-nm range. The total concentration of hemoglobin increases slightly with age, while for oxygen saturation there does not

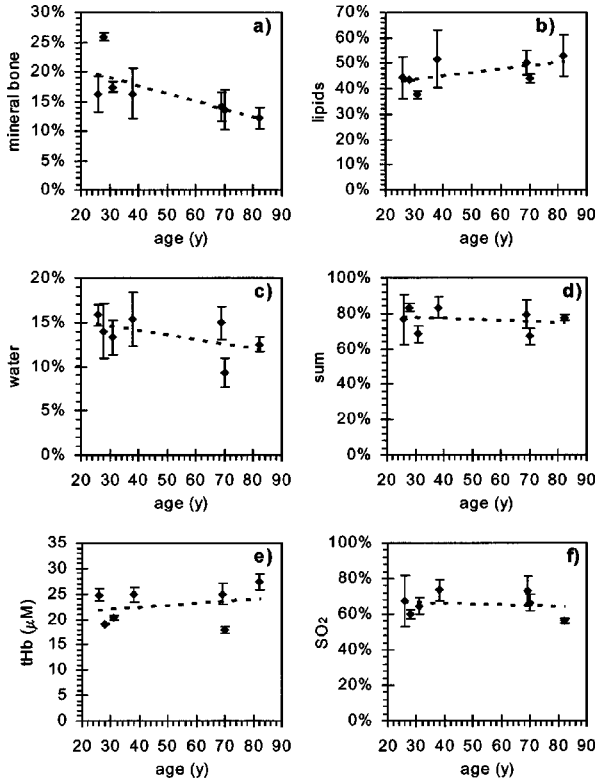

Fig. 6 Average estimate of (a) bone mineral matrix; (b) lipids; (c) water; (d) sum of water, lipids, and mineral bone contents; (e) tHb; and (f) SO_2 derived from the analysis of the absorption spectra.

seem to be a trend with age. All SO_2 values are within the typical physiological range for human tissues.

A clear problem visible in Fig. 6 is the large error bar associated with the measurements, which hampers a precise comparison of tissue composition. This uncertainty cannot be ascribed to the performance of the instrument since we have determined—on phantoms—a stability of the fitted spectral values within $\pm 1\%$ for spectral measurements repeated continuously over 2 h, and a day-to-day reproducibility of the spectra of 5%.[34] The positioning of the optical probe on the calcaneous is particularly critical, owing to the internal conformation of the bone and to the contamination by other more superficial tissues (skin, muscles, tendons). As in the case of DEXA, it is necessary to find an optimal positioning protocol to reduce intersubject variations. To reduce the uncertainties ascribed to the internal bone conformation, it could help to obtain a transmittance image of the region of interest once the optimal measurement wavelengths are known.

It is relevant to point out here that the theoretical model used for the analysis was derived for a homogeneous slab. The geometry is probably reflected in our measurements since the fibers were positioned in a rather flat region far from the boundaries. However, the hypothesis of a homogeneous medium cannot be applied to the superficial soft tissues covering the bone. The bone itself is probably almost homogeneous since the trabecular bone, unlike the cortical bone, is uniformly filled with bone marrow. Overall, the *in vivo* situation is much more complex than the simple media described by the theoretical model; thus the fitted optical properties are not an accurate estimate of the average coefficients, but they do keep track of the traversed bone and are sensitive to physiological changes in the bone composition.

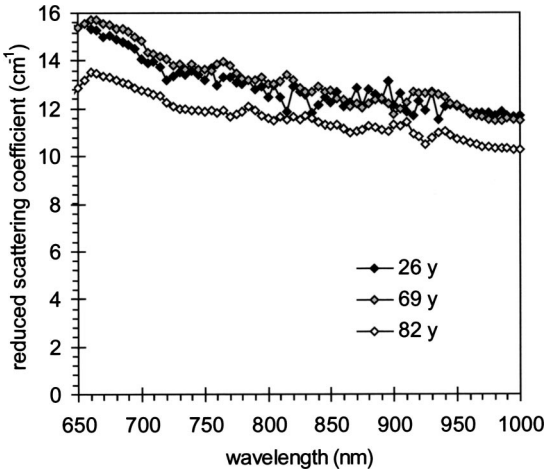

Fig. 7 Average reduced scattering spectra of the left calcaneous for the 26-, 69-, and 82-year-old volunteers.

Figure 7 presents the scattering spectra for the same three subjects considered in Fig. 4. Although the oldest volunteer presents the lowest scattering spectrum, the other two cases have quite overlapped spectra despite a large difference in age. The reduced scattering coefficient decreases with wavelength, from 14 to 16 to 10 to 12 cm^{-1}. The reduced scattering of both lipids and bone decreases slowly with wavelength, with similar spectral behavior, and that is possibly why the experimental curves for different subjects have similar slopes and absolute values, even though they correspond to different contents of lipids and bone. Figure 8 shows an example of a fit of the experimental data (white diamonds) with the theoretical expression derived from Eq. (2) (solid line) for the 31-year-old subject. The fit yields an estimated $b = 0.67$. The low b value is indicative of a slowly descending spectrum that is due to scattering centers of large effective size, similar to what we have already found in the case of adipose tissues.[35]

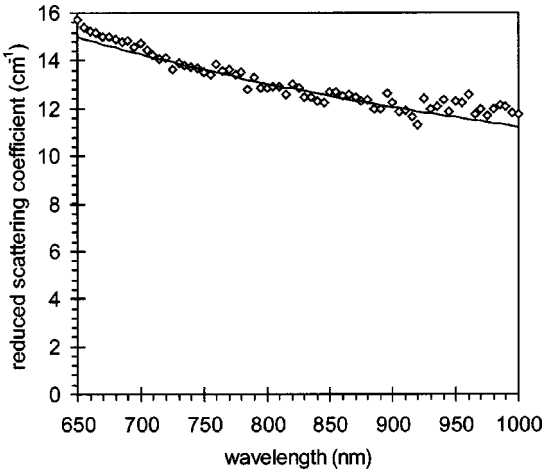

Fig. 8 Reduced scattering spectrum of the left calcaneous for the 31-year-old volunteer. Experimental data (diamonds) and theoretical curve (solid line) for using Mie theory.

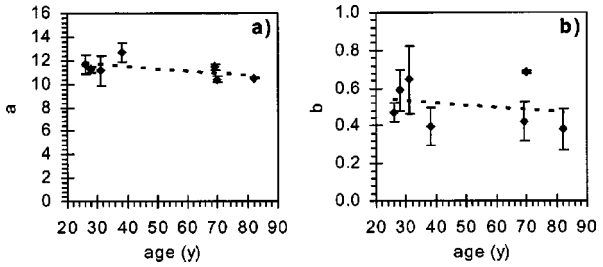

Fig. 9 Average estimate of (a) the Mie equivalent *a* and (b) *b* coefficients derived from the analysis of the scattering spectra.

The fitted values of the Mie-equivalent parameters *a* and *b* are shown for all subjects in Figs. 9(a) and 9(b), respectively. It is difficult to derive a definite trend for the *b* parameter, mainly because of the large intrasubject variation. The *a* value slightly decreases age, yet the trend is not so clear, and it is not obvious even when looking at the spectra of the seven volunteers. As already mentioned, a sound correlation was found between the scattering coefficient and the BMD on *ex vivo* pure mineral bone samples.[19] This is reasonable since the lower value of bone mineral density should correspond to a lower scattering. Yet, *in vivo*, the situation could be quite different since the progressive reduction of mineral matrix is compensated by an increase in lipid content that, as we have already noted, has a similar scattering power. Owing to these two competitive effects, the scattering coefficient of tissue would probably not be a valid indicator of bone structure, at least in this wavelength range. More data are needed to make a definite statement on this point.

4 Conclusions

In conclusion, we have shown the first *in vivo* TRS measurements of the human calcaneous over a broad spectral range. Absorption and scattering spectra were obtained for female volunteers of different ages. Analysis of the absorption properties led to the estimation of the concentration of the key tissue constituents. Older volunteers showed a lower percentage of bone mineral matrix, usually accompanied by a higher lipid and lower water content. Scattering spectra were less effective in indicating age-related changes, with a minor trend toward a decrease in the scattering coefficient. Clearly, we have not yet demonstrated a correlation between the TRS measurements and the BMD or generally the degree of osteoporosis as assessed by standard DEXA because of the unavailability of this information for most of the volunteers and the limited number of subjects. However, we have shown the applicability of the technique to an *in vivo* environment and its ability to probe tissue composition. There is some good evidence that this optical biopsy method could prove to be a useful tool for investigating pathological bone conditions in order to understand the progression of the disease and to diagnose osteopenia and osteoporosis. To this end, we plan to perform measurements on larger numbers of volunteers and to compare optical data with the results of the standard diagnostic technique (DEXA) for osteoporosis. In the case of positive results, we could develop a compact TRS instrument operating at discrete wavelengths up to 1000 nm that would be suitable for clinical application, as we have already demonstrated in the case of optical mammography, which involves a similar range of tissue thickness and optical properties.[36]

Acknowledgments

Ekaterine Chikoidze was supported by the ICTP Program for Training and Research in Italian Laboratories, Trieste, Italy.

References

1. National Osteoporosis Foundation, ''Osteoporosis: review of the evidence for prevention, diagnosis, and treatment and cost effective analysis,'' *Osteoporosis Int.* **8**, S1–S88 (1998).
2. D. Burr, M. Forwood, and D. Fyhire, ''Bone micro damage and skeletal fragility in osteoporotic and stress fractures,'' *J. Bone Miner. Res.* **12**, 6–16 (1997).
3. T. A. Einhorn, ''Bone strength: the bottom line,'' *Calcif. Tissue Int.* **51**, 333–339 (1992).
4. World Health Organization, ''Assessment of fracture risk and its application to screening for postmenopausal osteoporosis: report of a WHO study group,'' *World Health Org. Tech. Rep. Ser.* **843**, 1–129 (1994).
5. J. D. Kaufman, ''Osteoporosis: bone density tests,'' *Am. Acad. Orthopaed. Surg. Bull.* **47**, 33–35 (1999).
6. Y. Lu, H. K. Genant, J. Shepherd, S. Zhao, A. Mathur, T. P. Fuerst, and S. R. Cummings, ''Classification of osteoporosis based on bone mineral densities,'' *J. Bone Miner. Res.* **16**, 901–910 (2001).
7. M. D. Bracker and N. B. Watts, ''How to get the most out of bone densitometry. Results can help assess fracture risk and guide therapy,'' *Postgrad Med.* **104**, 77–86 (1998).
8. M. A. Parfitt, ''Interpretation of bone density measurements. Disadvantages of a percentage scale and a discussion of some alternatives,'' *J. Bone Miner. Res.* **5**, 537–540 (1990).
9. P. D. Miller, S. L. Bonnick, C. J. Rosen, R. D. Altman, L. V. Avioli, J. Dequeker, D. Felsenberg, H. K. Genant, C. Gennari, K. D. Harper, A. B. Hodsman, M. Kleerekoper, C. A. Mautalen, M. R. McClung, P. J. Meunier, D. A. Nelson, N. F. Peel, L. G. Raisz, R. R. Recker, W. H. Utian, R. D. Wasnich, and N. B. Watts, ''Clinical utility of bone mass measurements in adults: consensus of an international panel,'' *Semin Arthritis Rheum.* **25**, 361–372 (1996).
10. D. Marshall, O. Johnell, and H. Wedel, ''Meta-analysis of how well measures of bone mineral density predict occurrence of osteoporotic fractures,'' *Br. Med. J.* **18**, 1254–1259 (1996).
11. G. M. Blake, C. C. Gluer, and I. Fogelman, ''Bone densitometry: current status and future prospects,'' *Br. J. Radiol.* **70**, 177–186 (1997).
12. P. L. A. van Daele, H. Burger, C. E. D. H. De Laet, and H. A. P. Pols, ''Ultrasound measurement of the bone,'' *Clin. Endocrinol. (Oxford)* **44**, 363–369 (1996).
13. D. C. Bauer, C. C. Gluer, J. A. Cauley, T. M. Vogt, K. E. Ensrud, H. K. Genant, and D. M. Black, ''Broadband ultrasound attenuation predicts fractures strongly and independently of densitometry in older women. A prospective study of osteoporotic fractures group,'' *Arch. Intern. Med.* **157**, 629–634 (1997).
14. C. C. Gluer, S. R. Cummings, D. C. Bauer, K. Stone, A. Pressman, A. Mathur, and H. K. Genant, ''Osteoporosis: association of recent fractures with quantitative U.S. findings,'' *Radiology* **199**, 725–732 (1996).
15. American Medical Association, ''Managing osteoporosis part 1: detection and clinical issues in testing,'' (http://www.ama-assn.org/cmeselec).
16. S. Majumdar, P. Augat, J. C. Lin, D. Newitt, Y. Lu, N. E. Lane, and H. K. Genant, ''*In vivo* high-resolution MRI of the calcaneus: differences in trabecular structure in osteoporosis patients,'' *J. Bone Miner. Res.* **13**, 1175–1182 (1998).
17. Yong Xu, N. Iftimia, Huabei Jiang, L. L. Key, and M. B. Bolster, ''Three-dimensional diffuse optical tomography of bones and joints,'' *J. Biomed. Opt.* **7**, 88–92 (2002).
18. A. Schwaighofe, V. Tresp, P. Mayer, A. Krause, J. Beuthan, H. Rost, G. Metzger, G. A. Muller, and A. K. Scheel, ''Classification of rheumatoid joint inflammation based on laser imaging,'' *IEEE Trans. Biomed. Eng.* **50**, 375–382 (2003).
19. A. Takeuchi, R. Araki, S. G. Proskurin, Y. Takahashi, Y. Yamada, J. Ishii, S. Katayama, and A. Itabashi, ''A new method of bone tissue

measurement based upon light scattering,'' *J. Bone Miner. Res.* **12**, 261–266 (1997).
20. C. G. Kontoyannis and N. V. Vagenas, ''FT-Raman spectroscopy: a tool for monitoring the demineralization of bones,'' *Appl. Spectrosc.* **54**, 1605–1609 (2000).
21. M. S. Patterson, B. Chance, and B. C. Wilson, ''Time-resolved reflectance and transmittance for the noninvasive measurement of tissue optical properties,'' *Appl. Opt.* **28**, 2331–2336 (1989).
22. R. C. Haskell, L. O. Svasaand, T. T. Tsay, T. C. Feng, M. S. McAdams, and B. J. Tromberg, ''Boundary conditions for the diffusion equation in radiative transfer,'' *J. Opt. Soc. Am. A* **11**, 2727–2741 (1994).
23. K. Furutsu and Y. Yamada, ''Diffusion approximation for a dissipative random medium and the applications,'' *Phys. Rev. E* **50**, 3634–3640 (1994).
24. W. H. Press, S. A. Teukolsky, W. T. Vetterling, and B. P. Flannery, *Numerical Recipes in C: The Art of Scientific Computing*, Cambridge University Press, New York (1992).
25. S. Prahl, Oregon Medical Laser Center website: http://omlc.ogi.edu/spectra/water/index.html.
26. S. J. Matcher, C. E. Elwell, C. E. Cooper, M. Cope, and D. T. Delpy, ''Performance comparison of several published tissue near-infrared spectroscopy algorithms,'' *Anal. Biochem.* **227**, 54–68 (1995).
27. R. Cubeddu, A. Pifferi, P. Taroni, A. Torricelli, and G. Valentini, ''Non-invasive absorption and scattering spectroscopy of bulk diffusive media: an application to the optical characterization of human breast,'' *Appl. Phys. Lett.* **74**, 874–876 (1999).
28. C. F. Bohren and D. R. Hoffman, *Absorption and Scattering of Light by Small Particles*, Wiley, New York (1983).
29. J. R. Mourant, T. Fuselier, J. Boyer, T. M. Johnson, and I. J. Bigio, ''Predictions and measurements of scattering and absorption over broad wavelength ranges in tissue phantoms,'' *Appl. Opt.* **36**, 949–957 (1997).
30. A. O. Ugnell and P. A. Oberg, ''The optical properties of the cochlear bone,'' *Med. Eng. Phys.* **19**, 630–636 (1997).
31. M. Firbank, M. Hiraoka, M. Essenpreis, and D. T. Delpy, ''Measurement of the optical properties of the skull in the wavelength range 650–950 nm,'' *Phys. Med. Biol.* **38**, 503–510 (1993).
32. Genius, a division of Bomer S.p.A., www.genius.ind.br.
33. F. A. Duke, *Physical Properties of Tissue*, Academic Press, London (1990).
34. J. Swartling, A. Pifferi, E. Giambattistelli, E. Chikoidze, A. Torricelli, P. Taroni, M. Andersson, A. Nilsson, and S. Andersson-Engels, ''Rigorous characterization of time-resolved diffuse spectroscopy systems for measurements of absorption and scattering properties using solid phantoms,'' *Proc. SPIE* **5138**, 80–87 (2003).
35. A. Torricelli, A. Pifferi, P. Taroni, E. Giambattistelli, and R. Cubeddu, ''In vivo optical characterisation of human tissues from 610 to 1010 nm by time-resolved reflectance spectroscopy,'' *Phys. Med. Biol.* **46**, 2227–2237 (2001).
36. A. Pifferi, P. Taroni, A. Torricelli, F. Messina, R. Cubeddu, and G. Danesini, ''Four-wavelength time-resolved optical mammography in the 680 to 980 nm range,'' *Opt. Lett.* **28**, 1138–1140 (2003).